Temporal correlations versus noise in the correlation matrix formalism: An example of the brain auditory response

J. Kwapień,[1] S. Drożdż,[1,2] and A. A. Ioannides[3]
[1]*Institute of Nuclear Physics, PL–31-342 Kraków, Poland*
[2]*Institut für Kernphysik, Forschungszentrum Jülich, D-52425 Jülich, Germany*
[3]*Laboratory for Human Brain Dynamics, Brain Science Institute, RIKEN, Wako-shi, 351-0198, Japan*
(Received 14 February 2000; revised manuscript received 15 May 2000)

We adopt the concept of the correlation matrix to study correlations among sequences of time-extended events occurring repeatedly at consecutive time intervals. As an application we analyze the magnetoencephalography recordings obtained from the human auditory cortex in the epoch mode during the delivery of sound stimuli to the left or right ear. We look into statistical properties and the eigenvalue spectrum of the correlation matrix **C** calculated for signals corresponding to different trials and originating from the same or opposite hemispheres. The spectrum of **C** largely agrees with the universal properties of the Gaussian orthogonal ensemble of random matrices, with deviations characterized by eigenvectors with high eigenvalues. The properties of these eigenvectors and eigenvalues provide an elegant and powerful way of quantifying the degree of the underlying collectivity during well-defined latency intervals with respect to stimulus onset. We also extend this analysis to study the time-lagged interhemispheric correlations, as a computationally less demanding alternative to other methods such as mutual information.

PACS number(s): 87.19.Dd, 05.45.Tp, 05.40.−a

I. INTRODUCTION

Studying complex systems is typically based on analyzing large, multivariate data. Since, in general terms, complexity is primarily connected with coexistence of collectivity and chaos or even noise, it is of crucial importance to find an appropriate low dimensional representation of an underlying high dimensional dynamical system. In many cases this aims at denoising and compressing dynamic imaging data. Such a problem is particularly frequent in the area of the brain research where a complex but relatively sparse connectivity prevails. Understanding brain function requires a characterization and quantification of the correlations in the signals generated at different areas.

Direct pathways connect the sensory organs with the corresponding primary cortical areas. In the auditory system of interest here, delivery of a stimulus to either the left or the right ear is relayed to both primary auditory cortices, with stronger and earlier response on the contralateral side. The first cortical response arrives very early, well within 20 ms, but it is too weak to be mapped noninvasively from the outside. Successive waves of cortical activation follow with the strongest around 80–100 ms. For a simple stimulus and no cognitive task required the response as seen in the average is effectively over within the first 200–300 ms. More elaborate analysis shows that the ''echoic memory'' lasts for a few seconds [1,2]. Furthermore the activity in each area of the cortex, including the auditory cortex and its subdivisions, is determined by a plethora of interactions with other areas and not just the direct pathway from the cochlea. The variability of the evoked response possibly reflects the many ways a given input in the periphery can be modulated before the strong cortical activations emerge [3]. Our treatment of the activity from each auditory cortex as an independent signal bypasses this complexity by lumping many effects into information theoretic measures. The advantage of this approach is that it leads to quantitative analysis of stochastic and collective aspects of the complex phenomena in the auditory cortex and the brain at large.

In our previous work [4] we have established the existence of correlations between activity in the two auditory cortices, using mutual information [5] as a measure of statistical dependence. The analysis showed that collectivity and noise were present in the data [6].

Usually, one analyzes a set of simultaneously recorded signals which emerge from the activity of subcomponents of the system. Consequently, the presence of correlations in such signals is to be interpreted as a certain sort of cooperation among several or all of these sub-components. Though closely related, our present approach is somewhat different. Instead of studying many subsystems at the same time, we deal with two brain areas only and aim at identifying repetitive structures and their time relations in consecutive independent trials of delivery of the stimulus. We thus construct the correlation matrix (which is a normalized version of the covariance matrix [7,8]) whose entries express correlations among all the trials that are delivered by experiment. The difference relative to a conventional use of the correlation matrix is that now the indices of this matrix are labeling different presentations of the stimulus and not different subsystems. The resulting eigenspectrum is then expected to carry information about deterministic, nonrandom properties, separated out from the noisy background whose nature can also be quantified.

II. EXPERIMENT AND DATA

The details of the experiment can be found in our earlier articles [8,3,4]. Here, for completeness, we sketch briefly only the most important facts. Five healthy male volunteers participated in the auditory experiment. We used a

2×37-channel, two-dewar magnetoencephalography (MEG) apparatus (each dewar covered the temporal area in one hemisphere) to measure the magnetic field generated by the cortical electric activity [9]. The stimuli were 1 kHz tones lasting 50 ms each delivered in three runs to the left, right or both ears in 1 s intervals. The single trial of delivery of stimulus was repeated 120 times for each kind of stimulation. The cortical signals were sampled with 1042 Hz frequency. Pilot runs were used to place each dewar in turn so that both the positive and negative magnetic-field extrema were captured by the 37 channel array. With such a coverage it is feasible to construct linear combinations of the signals which act like virtual electrodes ''sensing'' the activity in the auditory cortex [3]. This computation can be done at each timeslice of each single trial independently, thus building the timeseries for each auditory cortex for further analysis [4].

Delivery of a sound stimulus or any change in the continuous stimulus causes a characteristic activity in the auditory cortex which is best illustrated by averaging many such events [10]. The (averaged) evoked potential, appears in both hemispheres and has a form of several positive and negative deflections of the magnetic field. The most prominent feature of the average is a high amplitude deflection at about 80–100 ms after the onset of the stimulus (so called M100). The details of the average evoked response are hardly visible in each single trial, partly because of strong background activity, which is not related to the stimulus and partly because of the latency jitter introduced by the many feed-forward and feed-back interactions that occur intermittently between the periphery and the cortex. If as the signal we consider what is fairly time locked to the stimulus onset, then the signal-to-noise ratio is much improved by averaging the signal over all single trials.

We will consider two runs, corresponding to stimuli delivered to the left and right ear. Each run comprises $N=120$ single trials, thus we have 120 signals for each hemisphere and each kind of stimulation. The signals are represented by the time series $x_\alpha^{L,R}(t_i)$ of length of $T=1042$ time slices ($i=1,\ldots,1042$, $\alpha=1,\ldots,120$) each evenly covering 1 s time interval. Since all the stimuli were provided in precisely specified equidistant instants of time, all the series can be adjusted so that the onset of each stimulus corresponds to the same time slice $i=230$. Each signal starts 220 ms before and ends 780 ms after the onset. A band pass filter was applied in the 1–100 Hz range.

For a simple auditory stimulus and no cognitive task associated with it, the average evoked response lasts for 200–300 ms; this is also reflected in our earlier mutual information study of the signals [4]. Since other parts of each series are associated with activity which is not time locked to the stimulus, the appearance of similar events in both hemispheres and across trials results in correlations that are much stronger in the first few hundred milliseconds. The presence of correlations and collectivity cannot be excluded *a priori* from other periods and it is therefore of considerable interest to compare two such intervals. We have settled on two such intervals, each with 250 timeslices: the first we call the evoked potential (EP) interval and it covers the first 250 timeslices after stimulus onset, i.e., 250 time slices ($i=231,480$) (2–241 ms); this is the period where the average signal is strong. The second interval we consider as baseline or background (B) and for this we choose the interval from 501 ms and ending 740 ms after the onset of the stimulus ($i=751,1000$). Since the time between stimuli is 1 s our choice avoids the time just before stimulus onset, when anticipation and expectation is high while being as far as possible from the stimulus onset.

III. CORRELATION MATRIX ANALYSIS

For the two time series $x_\alpha(t_i)$ and $x_\beta(t_i)$ of the same length, ($i=1,\ldots,T$) one defines the correlation function by the relation

$$C_{\alpha,\beta}=\frac{\sum_i [x_\alpha(t_i)-\overline{x_\alpha}][x_\beta(t_i)-\overline{x_\beta}]}{\sqrt{\sum_i [x_\alpha(t_i)-\overline{x_\alpha}]^2 \sum_j [x_\beta(t_j)-\overline{x_\beta}]^2}}, \tag{1}$$

where $\overline{x}$ denotes a time average over the period studied. For two sets of N time series $x_\alpha(t_i)$ each ($\alpha,\beta=1,\ldots,N$) all combinations of the elements $C_{\alpha,\beta}$ can be used as entries of the $N\times N$ correlation matrix **C**. By diagonalizing **C**

$$\mathbf{C}\mathbf{v}^k=\lambda_k\mathbf{v}^k, \tag{2}$$

one obtains the eigenvalues λ_k ($k=1,\ldots,N$) and the corresponding eigenvectors $\mathbf{v}^k=\{v_\alpha^k\}$.

In the limiting case of entirely random correlations the density of eigenvalues $\rho_C(\lambda)$ defined as

$$\rho_C(\lambda)=\frac{1}{N}\frac{dn(\lambda)}{d\lambda}, \tag{3}$$

where $n(\lambda)$ is the number of eigenvalues of **C** less than λ, is known analytically [11], and reads

$$\rho_C(\lambda)=\frac{Q}{2\pi\sigma^2}\frac{\sqrt{(\lambda_{max}-\lambda)(\lambda-\lambda_{min})}}{\lambda}. \tag{4}$$

Here

$$\lambda_{min}^{max}=\sigma^2(1+1/Q\pm2\sqrt{1/Q}) \tag{5}$$

with $\lambda_{min}\leqslant\lambda\leqslant\lambda_{max}$, $Q=T/N\geqslant1$, and where σ^2 is equal to the variance of the time series (unity in our case). Interesting is both a potential agreement of our calculated eigenspectrum of **C** with this formula as well as deviations. In fact the deviations are even more interesting because they can be used to quantify certain system specific nonrandom properties of the system.

For our present detailed numerical analysis we select two characteristic subjects (DB and FB) out of all five subjects who participated in the experiment. The background activity in both subjects does not reveal any dominant rhythm which, if present in two signals, may introduce additional, spontaneous correlations not related to the stimulus. The signals of DB reveal relatively strong EP's and a good signal-to-noise ratio (SNR). FB is somehow on the other side of the spectrum of subjects, as its EP's are small and hardly visible and the signals are dominated by a high-frequency noise which results in a poor SNR. The signals forming pairs in Eq. (1)

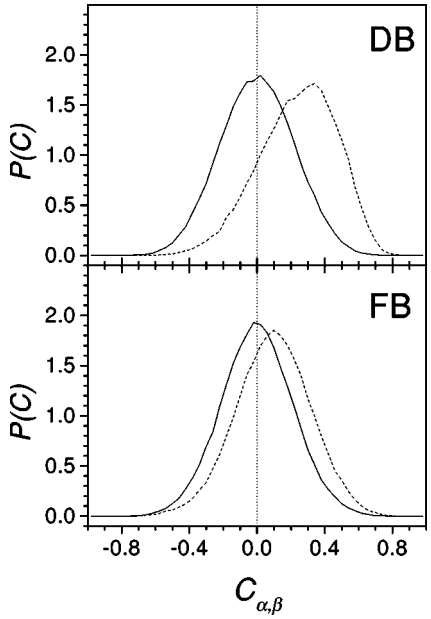

FIG. 1. Distributions of $C_{\alpha,\beta}$ for the one-hemisphere correlation matrix. The upper panel corresponds to DB and the lower one to FB. The solid lines display such distributions evaluated in the regions beyond evoked activity (B) and the dashed lines in the EP region.

may come either from the same or from the opposite hemispheres. The first possibility we term the *one-hemisphere* correlation matrix and the latter one is the *cross-hemisphere* correlation matrix. The first matrix is, by definition, real symmetric and the second one must be real but, in general, it is not symmetric.

An interesting global characteristic of the dynamics encoded in **C** is provided by the distribution of its elements. An example for such a distribution is shown in Fig. 1 for the one-hemisphere correlation matrix. As one can see in the background region (solid lines) the distributions are Gaussian-like centered at zero. This implies that the corresponding signals are statistically independent to a large extent. A significantly different situation is associated with the evoked potential part of the signal. The most obvious effect is that the center of mass of the distribution is shifted towards the positive values. In this respect there is also a difference between the subjects: the average value of the elements for DB (approximately 0.35) is considerably higher than for FB (0.05). This indicates that the signals in FB are on average less correlated even in the EP region than the signals recorded from DB. This may originate from either a smaller amplitude of the collective response of FB's cortex or from a much smaller signal-to-noise ratio. For the cross-hemisphere correlation matrix the relevant characteristics are similar. The only difference is that the shifts (in both subjects) are slightly smaller.

More specific properties of the correlation matrix can be analyzed after diagonalizing **C**. The one-hemisphere correlation matrix is real and symmetric and consequently all its eigenvalues are real. The structure of their distribution is displayed in Fig. 2. The eigenvalues are shown for several characteristic cases: two subjects, the left and right hemispheres and two regions (EP and B).

The structure of the eigenvalue spectra depends on the

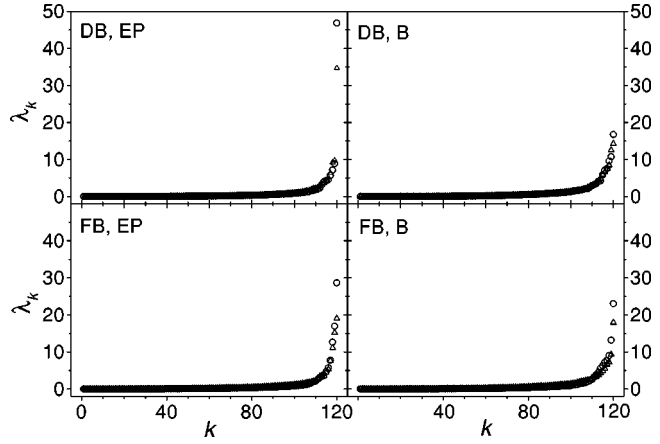

FIG. 2. Structure of the eigenvalue spectra of the correlation matrices (one-hemisphere correlations) for the two discussed regions of the signals (evoked potential - EP, background activity - B) for DB (upper part) and FB (lower part). In each panel there are two spectra of eigenvalues, corresponding to the right hemisphere (circles) and the left one (triangles). The eigenvalues are ordered from the smallest to the largest.

subject but first of all on the region of the signal. There is a clear separation of the largest eigenvalue from the rest of the spectrum in the EP region in DB. This effect is much less pronounced for FB and considerably reduced in B. This is consistent with the distribution of the corresponding matrix elements as shown in Fig. 1. To a first approximation the distribution of such elements in EP can be described as a shifted Gaussian [12]:

$$\mathbf{C} = \mathbf{G} + \gamma \mathbf{U}, \tag{6}$$

where **G** denotes a Gaussian matrix centered at zero and **U** is a matrix whose entries are all unity. γ is a real number $0 \leqslant \gamma \leqslant 1$. Of course, the rank of **U** is one and, therefore, the second term alone in Eq. (6) develops only one nonzero eigenvalue of magnitude γ. Since the expansion coefficients of this particular state are all equal this assigns a maximum of collectivity to such a state. If γ is significantly larger than zero the structure of **C** is predetermined by the second term in Eq. (6). As a result the spectrum of **C** comprises one collective state with large eigenvalue. Since in this case **G** constitutes only a ''noise'' correction to γ**U** all the other states are connected with significantly smaller eigenvalues. From the point of view of the analysis performed here the first component of Eq. (6) corresponds to an irrelevant signal. This may actually be noise, although it could easily be background activity not related to the stimulus, or even activity related to the processing of the stimulus but in a rather distinct and different way for each trial. The second term of Eq. (6) corresponds to activity time locked to the stimulus onset in each single trial. Since the center of mass of the distribution of matrix elements is shifted more towards the positive values for DB (and thus γ is larger) than for FB, the largest eigenvalue is significantly larger in the former case. Within the conventional spatiotemporal description based on the correlation matrix similar characteristics of collectivity have recently been identified [12] in correlations among companies on the stock market.

In relation to Eq. (4) the presence of a strongly separated eigenvalue is one obvious deviation which is consistent with the nonrandom character of the corresponding eigenstate. Further deviations can be identified by comparing the boundaries of our calculated spectrum to λ_{min}^{max} of Eq. (5). For $Q=T/N=250/120$ we obtain $\lambda_{min}=0.944$ and $\lambda_{max}=2.866$. Clearly, there are several more eigenvalues which are larger than λ_{max}. This may indicate that the corresponding eigenstates absorb a fraction of the collectivity. However, a closer inspection shows that also on the other side of the spectrum there are eigenvalues smaller than λ_{min} and basically no empty strip between 0 and λ_{min} can be seen. By this our empirical distribution seems to indicate that an effective Q which determines this distribution is significantly smaller than $Q=T/N$. This, in turn, may signal that the information content in the time series of length T is equivalent to a significantly shorter time series. This conclusion is supported by the time dependence of the autocorrelation function calculated [6] from our signals. It drops down relatively slowly and reaches zero only after 20–30 time steps between consecutive recordings. Memory effects are present and hence neighboring recordings during the same trial are not entirely independent and this also applies to components which reflect the background activity. It is well known that neural activity is characterized by a set of finite correlation times, and the suggestion has been made that continuity of awareness is quantized in a hierarchy of temporal scales [13]. The time scale of 25 ms, corresponding to 40 Hz, or γ band activity has been proposed as a fundamental unit (of memory): synchronized neural activity within and across brain areas, like the auditory cortex and its subdivisions, are combined to represent a unified perception even if elicited by different segments or aspects of an object. This requires the maintenance of an active state for this amount of time and hence naturally leads to the correlations that our data imply. On the hardware side there are plenty of time-delayed processes and interactions in the neuronal circuits of the brain which will produce activity in neighboring times with shared information. It is interesting to note that there exist eigenvalues larger than λ_{max} (and smaller than λ_{min} as well) also in the B region for both subjects even though the distribution of $C_{\alpha,\beta}$ is perfectly Gaussian in this case. This indicates the existence of further correlations among the matrix elements of **C** that are of different origin than those which can be quantified in simple terms of Eq. (4).

One could explicitly test the related role of memory effects by recomputing **C** with appropriately sparser time series. Unfortunately, the number of recordings covering the single trial is too small for a systematic study of such effects. Instead we perform the following analysis: we generate the new time series $d_\alpha(t_i)$ such that $d_\alpha(t_i)=x_\alpha(t_{i+1})-x_\alpha(t_i)$, i.e., the time series of differences. These destroy the memory effects and now the autocorrelation function drops down very fast. Figure 3 shows the density of eigenvalues of the correlation matrix generated from $d_\alpha(t_i)$. Now the agreement with Eq. (4) improves and becomes relatively good even in the EP region already when every second time point i from $d_\alpha(t_i)$ is taken, such that the total number of them remains the same ($T=250$). Taking more distant points, leaving out intermediate ones, drastically reduces the correlation between the remaining successive points. The above thus illustrates the subtleties connected with the correlation matrix analysis of time series. Replacing our original time series $x_\alpha(t_i)$ by $d_\alpha(t_i)$ improves the agreement with Eq. (4) and even the collective state connected with EP dissolves. This is due to the disappearance in $d_\alpha(t_i)$ of the memory effects present in $x_\alpha(t_i)$. On the level of d_α the correlations are thus essentially purely random and therefore, in the following, we return to our original time series.

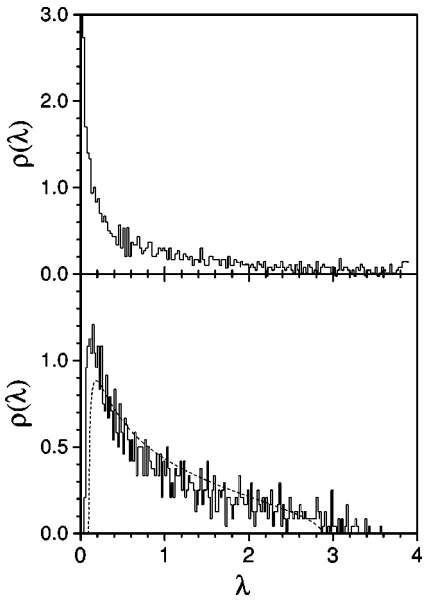

FIG. 3. Density of eigenvalues of the correlation matrix calculated from the $T=250$ points of the time series $d_\alpha(t_i)$ of increments of the original time series $x_\alpha(t_i)$, i.e., $d_\alpha(t_i)=x_\alpha(t_{i+1})-x_\alpha(t_i)$. In the lower panel every second point of $d_\alpha(t_i)$ is taken but the number of such points is still 250. The dashed line corresponds to the distribution prescribed by Eq. (4).

Another statistical measure of spectral fluctuations is provided by the nearest-neighbor spacing distribution $P(s)$. The corresponding spacings $s=\lambda_{i+1}-\lambda_i$ are computed after renormalizing the eigenvalues in such a way that the average distance between the neighbors equals unity. A related procedure is known as unfolding [14–16]. Two characteristic and typical examples of such distributions corresponding to EP and B regions are shown in Fig. 4 (for DB). While in both cases these distributions agree well with the Wigner distribution which corresponds to the Gaussian orthogonal ensemble (GOE) of random matrices, some deviations on the level of larger distances between neighboring states are more visible in the EP than in the B region. This in fact is consistent with the presence of larger eigenvalues in the EP case as shown in Fig. 2. Interestingly, the bulk of $P(s)$ even here agrees well with GOE. In order to further quantify the observed deviations we also fitted the histograms with the so-called Brody distribution

$$P_r(s)=(1+r)as^r\exp(-as^{(1+r)}), \tag{7}$$

where $a=[\Gamma((2+r)/(1+r))]^{1+r}$. Depending on a value of the repulsion parameter r, this distribution describes the intermediate situations between the Poisson (no repulsion, $r=0$) and the standard Wigner ($r=1$) distribution (GOE). The best fit in terms of Eq. (7) gives $r=0.95$ in the EP and

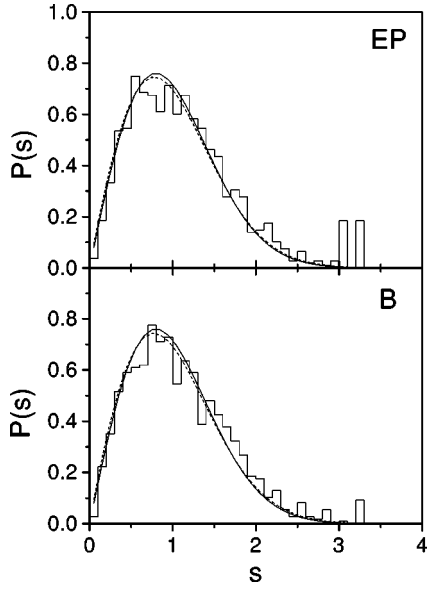

FIG. 4. Nearest-neighbor (s) spacing distribution (histogram) of the eigenvalues of **C** for subject DB. The upper panel corresponds to the evoked potential (EP) region of the time series and the lower panel to the background (B) activity part. The distributions have been created after unfolding the eigenvalues. The smooth solid curves illustrate the Wigner distribution and the dashed curves are the best fit in terms of the Brody distribution.

$r=0.93$ in the B case, respectively. Thus we clearly see that on the level of the nearest-neighbor spacing distribution $P(s)$ the original measurements share the universal properties of GOE. Here, similarly as in strongly interacting Fermi systems [17], $P(s)$ thus proves more robust against correlations than the dependences expressed by Eq. (4). A departure betraying some collectivity is nevertheless present in both B and EP intervals, but even in the EP interval the effect of the stimulus does not change this picture significantly: it results in one or at most a few remote distinct states in the sea of low eigenvalues of the GOE type.

In order to further explore this effect we look at the distribution of the eigenvector components v_α^k for the same cases as in Fig. 4. Figure 5 displays such a distribution generated from eigenvectors associated to one hundred lowest eigenvalues (main panels of the Figure) calculated both for the EP (upper part) and B (lower part) regions. The result is a perfectly Gaussian distribution in both cases. However, in EP a completely different distribution (upper inset) corresponds to the state with the largest eigenvalue. The characteristic peak located at around 0.1 documents that the majority of the trials contribute to this eigenvector with similar strength. This eigenvector is thus associated with a typical behavior of many single-trial signals. The component values in the largest eigenvalue in B also deviate from a Gaussian distribution (inset in the lower part of Fig. 5), although in this case their distribution is largely symmetric with respect to zero. This makes the two $k=120$ eigenvectors in B and EP regions approximately orthogonal which indicates a different mechanism generating collectivity in these two regions.

A more explicit way to visualize the differences among the eigenvectors is to look at the superposed signals

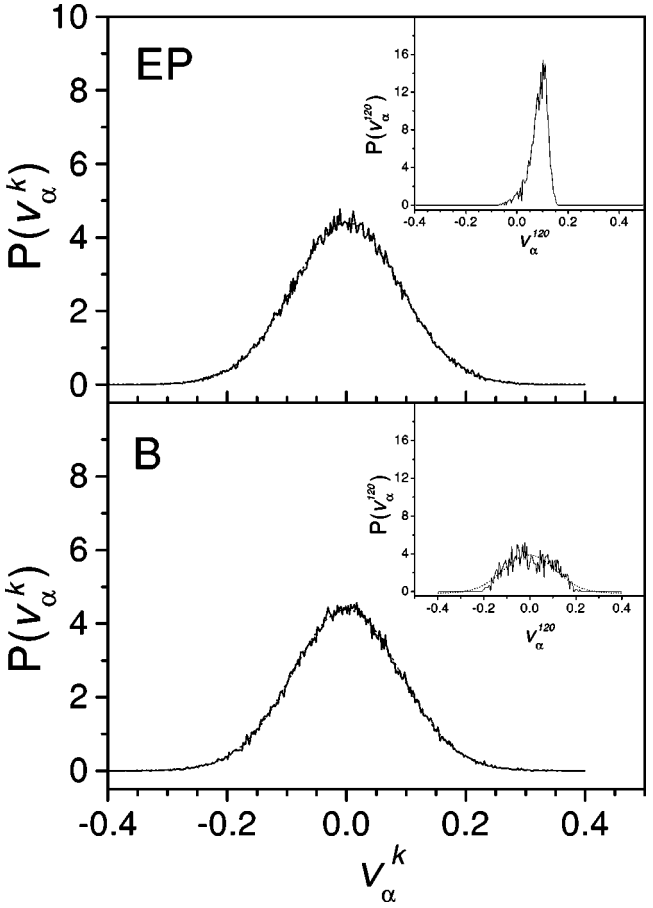

FIG. 5. Distribution of the eigenvector components (v_α^k) for EP (upper part) and B (lower part) regions (subject DB). The main panels correspond to one hundred lowest eigenvalues, while the insets show plots of the same quantity for the eigenvector corresponding to λ_{max} ($k=120$). For comparison, Gaussian best fits are also presented (dotted lines). (Note different scales in the figure.)

$$x_{\lambda_k}(t_i)=\sum_{\alpha=1}^{120} v_\alpha^k x_\alpha(t_i). \tag{8}$$

For $k=120$, 119, and 75 these are shown in Fig. 6 using the eigenvectors calculated for the EP (middle panel) and for B (lower panel) regions. The signals corresponding to the largest eigenvalues ($k=120$) develop the largest amplitudes in both cases. In the first case (EP) it very closely resembles a simple average (upper panel) over all the trials. In the second case (B) the largest eigenvalue also shows a degree of collectivity even though the corresponding simple average develops no coherent structure. Also, when signals weighted by the eigenvectors with the highest eigenvalue in EP and B are compared we see that there is essentially no amplification in the other region (i.e., in the EP interval when the B-weighted signals are used). In addition, keeping in mind in this connection both the difference in distribution of $C_{\alpha,\beta}$ in EP and B (Fig. 1), respectively, and the asymmetry (EP) versus symmetry (B) in the distribution of the largest eigenvector components (insets to Fig. 5), which makes the two eigenvectors approximately orthogonal, this provides another indication that different mechanisms are responsible for the collectivity at these two different latency ranges. Analogous effects of

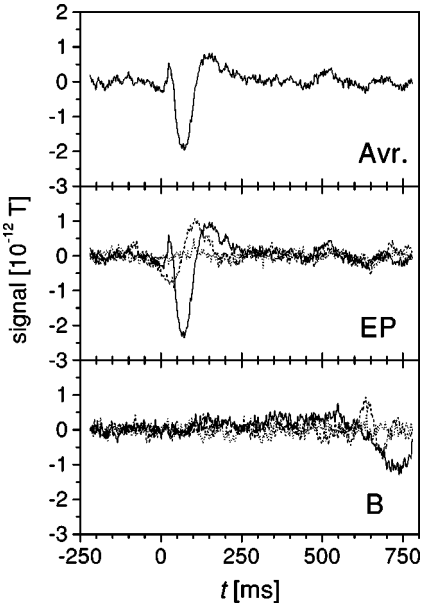

FIG. 6. The comparison of the signal obtained by the simple average over all 120 trials (upper panel) and the signals obtained from Eq. (8) for both regions, EP (middle part) and B (lower part) for subject DB. Signals in the middle and lower panels denote superpositions for $k=120$ (solid line), $k=119$ (dashed line), and $k=75$ (dotted line).

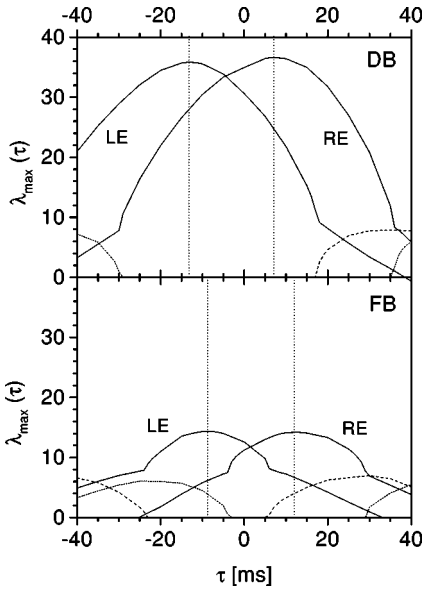

FIG. 7. $\lambda_{max}(\tau)$ calculated from the cross-hemisphere correlation matrix. The upper part corresponds to DB and the lower part to FB. Both panels illustrate two kinds of stimulation: left ear (LE) and right ear (RE). The solid lines denote the real part of λ_{max}, while the dashed and dotted ones are its imaginary part. The sign of τ denotes retardation of a signal from the right hemisphere ($\tau>0$) or the left one ($\tau<0$).

collectivity for $k=119$ are already much weaker and disappear completely as an example of $k=75$ shows.

We now turn to the cross-hemisphere correlation function, obtained by forming pairs in Eq. (1) from the time series representing opposite hemispheres [$x^L_\alpha(t_i)$ with $x^R_\beta(t_i)$]. Introducing in addition a time-lag τ between such signals [4], and dropping the rather obvious superscripts for the left and right hemisphere, we define a delayed correlation matrix

$$C_{\alpha,\beta}(\tau)=\frac{\sum_i [x_\alpha(t_i)-\overline{x_\alpha}][x_\beta(t_i+\tau)-\overline{x_\beta}]}{\sqrt{\sum_i [x_\alpha(t_i)-\overline{x_\alpha}]^2 \sum_j [x_\beta(t_j+\tau)-\overline{x_\beta}]^2}},$$

$$\alpha,\beta=1,\ldots,N. \tag{9}$$

A similar cross-correlation time-lag function has been employed in the past to investigate across trials correlations, but because of the high computational load of an exhaustive comparison across different delays the analysis was restricted to the computation of the time-lagged cross-correlation between the average and individual single trials [8]. The spectral decomposition of the cross-correlation matrix provides a more elegant approach, requiring the solution of the τ-dependent eigenvalue problem

$$\mathbf{C}(\tau)\mathbf{v}^k(\tau)=\lambda_k(\tau)\mathbf{v}^k(\tau), \quad k=1,\ldots,N. \tag{10}$$

Since $\mathbf{C}$ can now be asymmetric its eigenvalues λ_k can be complex (but forming pairs of complex conjugate values since $\mathbf{C}$ remains real) and in our case they generically are complex indeed. One anticipated exception may occur when the similarity of the signals in both hemispheres takes place for a certain value of τ. In this case $\mathbf{C}$ is dominated by its symmetric component and the effect, if present, is thus expected to be visible predominantly on the largest eigenvalue. It is more likely to see this effect in the EP region of the time series. We thus calculate the cross-hemisphere correlation matrix from the $T=250$-long subintervals of $x^L_\alpha(t_i)$ and $x^R_\beta(t_i)$ covering the EP's. Figure 7 presents the resulting real and imaginary parts of the largest eigenvalue as a function of τ for two subjects and two kinds of stimulation (left and right ear). As it is clearly seen the large real parts are accompanied by vanishing imaginary parts. Based on this figure several other interesting observations are to be made. First of all $\lambda_{max}(\tau)$ strongly depends on τ and reaches its maximum for a significantly nonzero value of τ. This reflects the already known fact [4] that the contralateral (opposite to the side the stimulus is delivered) hemisphere responds first and thus the maximum of synchronization occurs when the signals from the opposite hemispheres are shifted in time relative to each other. (Here $\tau>0$ means that the signal from the right hemisphere is retarded relative to the left hemisphere and the opposite applies to $\tau<0$.) Furthermore, the magnitude ($\tau\sim10$ ms) of the time delay estimated from locations of the maxima agrees with an independent estimate based on the mutual information [4]. Even a stronger degree of synchronization for DB relative to FB, as can be concluded from a significantly larger value of λ_{max} in the former case, agrees with this previous study.

Finally, Fig. 8 shows some examples of the eigenvalue distribution on the complex plane. In the EP region the specific value of the time delay ($\tau=7$ ms, upper panel) corresponds to maximum synchronization between the two hemispheres for this particular subject. Here we see one strongly repelled eigenvalue with a large real part (~36.5) and a

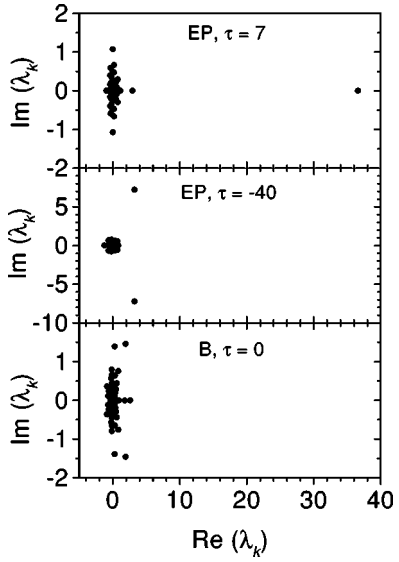

FIG. 8. Examples of the eigenvalue distribution of the cross-hemisphere correlation matrix for the right ear stimulation for DB obtained from the EP region (upper and middle panels) and the B region (lower panel). All parts present the distributions on the complex plane. The eigenvalues for $\tau=7$, which corresponds to the maximum of $\lambda_{max}(\tau)$ in Fig. 7, are shown in the upper panel and the eigenvalues for $\tau=-40$ (corresponding to strong antisymmetry of **C**) are presented in the middle one. A typical distribution of the eigenvalues in the B region is illustrated in the lower part. (Note different scale in the middle panel.)

vanishing imaginary part. An interesting sort of collectivity can be inferred from an example shown in the middle panel ($\tau=-40$ ms) of Fig. 8. Here the largest eigenvalue is about a factor of 3 repelled more in the imaginary axis direction than in the real direction. This indicates that the antisymmetric part of **C** is dominating it which expresses certain effects of antisynchronization (synchronization between the signals opposite in phase). In the B region, on the other hand, there are basically no such effects of synchronization between the two hemispheres and, consequently, the complex eigenvalues are distributed more or less uniformly around (0,0) as an example in the lowest panel of Fig. 8 shows.

IV. CONCLUSIONS

The standard application of the correlation matrix formalism is to study correlations among (nearly) coincident events in different parts of a given system. A typical principal aim of the related analysis is to extract a low-dimensional, non-random component which carries some system specific information from the whole multidimensional background activity. The advantage of the correlation matrix formalism is that it allows us to directly relate the results to universal predictions of the theory of random matrices. In the present study we have used the correlation matrix as a tool for analyzing single trial responses, treating the time series of each single trial as a separate system element. A dendrogram description of the distribution of auditory evoked MEG responses in single trials has demonstrated that single trials partition into sets, with each set possibly reflecting a different anatomical route from the ear to the auditory cortex [3]. Consistently, in the present approach the spectrum separates into the background of noise eigenvalues and a group of eigenstates with large eigenvalues. The distribution of eigenvector components associated to the highest eigenvalue in EP is ordered towards high correlations with almost no negative values and a sharp distribution. This implies that the trials quite systematically involve a component prescribed by this eigenvector. This is in agreement with earlier findings [3], but now it comes directly from the time series of single trials without any processing and artificial partition into groups of trials. In addition, the correlation matrix approach enabled us to quantify the nature of the background brain activity at long latencies (B), where the precise time locking is lost but a measure of collectivity remains. The mechanism responsible for this collectivity appears different from that for EP, but it is not clear whether this is because the time locking to stimulus onset is relaxed or because of a truly new neuronal mechanisms. In any case for both EP and B periods the results are largely consistent with the Gaussian orthogonal ensemble of random matrices: the introduction of the stimulus leads to a small perturbation of the background state, again a result echoing the conclusion of [3], but now reached within a firmer and better understood mathematical framework. The analysis offers a way of comparing the degree of collectivity from the properties of the eigenvectors with the highest eigenvalues, and crucially to quantify the degree of collectivity. The beginnings of how the method can be extended to study correlations between the two sources of signals was also outlined. In this case the correlation matrix is asymmetric and results in complex eigenvalues. An immediate application of such an extension is to look at correlations among signals recorded in our experiment from the opposite hemispheres. Introducing in addition the time lag between the signals one can study the effects of delayed synchronization between the two hemispheres. The quantitative characteristics of such synchronization remain in agreement with those found by other means [4].

[1] Z.L. Lü, S.J. Williamson, and L. Kaufman, Science **258**, 1668 (1992).
[2] L.C. Liu, A.A. Ioannides, and J.G. Taylor, Neuroreport **9**, 2679 (1998).
[3] L.C. Liu, A.A. Ioannides, and H.W. Müller-Gärtner, Electroencephalogr. Clin. Neurophysiol. **106**, 64 (1998).
[4] J. Kwapień, S. Drożdż, L.C. Liu, and A.A. Ioannides, Phys. Rev. E **58**, 6359 (1998).
[5] A.M. Fraser and H.L. Swinney, Phys. Rev. A **33**, 1134 (1986).
[6] S. Drożdż, J. Kwapień, A.A. Ioannides, and L.C. Liu, in *Collective Excitations in Fermi and Bose Systems*, edited by C.A. Bertulani, L.P. Canto, and M.S. Hussein (World Scientific, Singapore, 1999), pp. 62–77.
[7] D.S. Broomhead and G.P. King, Physica D **20**, 217 (1986).
[8] L.C. Liu and A.A. Ioannides, Brain Topogr. **8b(4)**, 385 (1996).
[9] M. Hämäläinen, R. Hari, R.J. Ilmoniemi, J. Knuutila, and O. Lounasmaa, Rev. Mod. Phys. **65**, 413 (1993).
[10] O.D. Creutzfeldt, *Cortex Cerebri* (Oxford University Press,

Oxford, 1995).
[11] A. Edelman, SIAM J. Matrix Anal. Appl. **9**, 543 (1988); A.M. Sengupta and P.P. Mitra, Phys. Rev. E **60**, 3389 (1999).
[12] S. Drożdż, F. Grümmer, F. Ruf, and J. Speth, e-print cond-mat/9911168.
[13] E. Poeppel, Trends Cogn. Sci. **1**, 56 (1997).
[14] T.A. Brody, J. Flores, J.B. French, P.A. Mello, A. Panday, and S.S.M. Wong, Rev. Mod. Phys. **53**, 385 (1981).
[15] M.L. Mehta, *Random Matrices* (Academic, Boston, 1991).
[16] S. Drożdż and J. Speth, Phys. Rev. Lett. **67**, 529 (1991).
[17] S. Drożdż, S. Nishizaki, J. Speth, and J. Wambach, Phys. Rev. C **49**, 867 (1994); S. Drożdż, S. Nishizaki, J. Speth, and M. Wójcik, Phys. Rev. E **57**, 4016 (1998).